Environmental Science & Technology

Article

Cite This: Environ. Sci. Technol. 2018, 52, 14480−14486

pubs.acs.org/est

Uptake, Whole-Body Distribution, and Depuration of Nanoplastics by the Scallop *Pecten maximus* at Environmentally Realistic Concentrations

Maya Al-Sid-Cheikh,*[,†] Steve J. Rowland,[‡] Karen Stevenson,[§] Claude Rouleau,[∥] Theodore B. Henry,[⊥] and Richard C. Thompson*[,†]

[†]School of Biological and Marine Sciences, University of Plymouth, Drake Circus, Plymouth, PL4 8AA, United Kingdom

[‡]School of Geography, Earth and Environmental Sciences, University of Plymouth, Drake Circus, Plymouth, PL4 8AA, United Kingdom

[§]Charles River, Elpinstone Research Centre, Elphinstone, Tranent EH33 2NE, United Kingdom

[∥]Institut des Sciences de la Mer de Rimouski (ISMER), Université du Québec à Rimouski, 310 allée des Ursulines, Rimouski, Québec Canada G5L 3A1

[⊥]Institute of Life and Earth Sciences Heriot-Watt University, John Muir Building, Edinburgh, EH14 4AS, United Kingdom

Supporting Information

ABSTRACT: Previous studies of uptake and effects of nanoplastics by marine organisms have been conducted at what may be unrealistically high concentrations. This is a consequence of the analytical challenges in tracking plastic particles in organisms at environmentally relevant concentrations and highlights the need for new approaches. Here, we present pulse exposures of ^{14}C-radiolabeled nanopolystyrene to a commercially important mollusk, *Pecten maximus*, at what have been predicted to be environmentally relevant concentrations (<15 μg L^{-1}). Uptake was rapid and was greater for 24 nm than for 250 nm particles. After 6 h, autoradiography showed accumulation of 250 nm nanoplastics in the intestine, while 24 nm particles were dispersed throughout the whole-body, possibly indicating some translocation across epithelial membranes. However, depuration was also relatively rapid for both sizes; 24 nm particles were no longer detectable after 14 days, although some 250 nm particles were still detectable after 48 days. Particle size thus apparently influenced the biokinetics and suggests a need for chronic exposure studies. Modeling extrapolations indicated that it could take 300 days of continued environmental exposure for uptake to reach equilibrium in scallop body tissues although the concentrations would still below 2.7 mg g^{-1}. Comparison with previous work in which scallops were exposed to nonplastic (silver) nanomaterials of similar size (20 nm), suggests that nanoparticle composition may also influence the uptake tissue distributions somewhat.

INTRODUCTION

Plastics are lightweight, inexpensive, and highly durable materials that are used in a wide variety of products, which have contributed to almost every aspect of modern life, displacing other materials and revolutionizing contemporary society. In 2016, global plastics production totaled around 335 million metric tons, around 40% of which was in single-use products that are discarded rapidly.[1] Consequently, considerable quantities of end-of-life plastics have accumulated as waste in managed systems and as litter in the environment. Once in the environment, exposure to ultraviolet light can cause plastics to become brittle and then fragment by mechanical action, leading to the formation of microscopic pieces, sometimes known as microplastics (MP).[2] It is estimated that up to 51 trillion microplastic fragments have accumulated at the sea surface and that quantities are increasing.[3] It has been widely suggested that this fragmentation will eventually result in the formation of plastic nanoparticles (NP). Current analytical approaches limit the ability to isolate and identify nanoparticles from environmental media. However, there is some experimental evidence to indicate the potential for nanoparticles to have accumulated in the environment. For example, Koelmans et al.[4] (2015) reported fragmentation of expanded polystyrene (EPS) to micro- and nanosize pieces in experiments involving a month of accelerated mechanical abrasion with glass beads and sand. Some other laboratory studies have also identified the presence

Received: September 18, 2018
Revised: November 16, 2018
Accepted: November 20, 2018
Published: November 20, 2018

of plastics at the nanoscale in water, after exposure of larger plastics pieces to UV and visible radiation.[5,6] Given the current rate of entry of plastic litter to the environment the potential for substantial long-term accumulation of nanoplastic fragments seems high. In addition, a range of nanoplastic particles are manufactured for commercial applications, including in paints, adhesives, coatings, biomedical products, electronics,[7] and cosmetics;[8] it seems likely that some of these manufactured nanoparticles will also be released to the environment.

A number of studies, all of which are laboratory based, have investigated either the uptake or effects of nanoplastics on a range of marine organisms. The majority have used concentrations exceeding by two to seven orders-of-magnitude, those predicted to occur in the environment (e.g., ref 3, SI Figure S1 and associated references). Predicted environmental concentrations, which are likely to increase exponentially as the particle size decreases are, for example, 1 pg L^{-1} to 15 μg L^{-1} (μg L^{-1} = parts per billion, ppb) for ~50 nm and below 0.5 μg L^{-1} for 5 μm plastic particles.[9] Concentrations are likely to be higher in environmental compartments where there is some degree of plastic particle accumulation.

A first step toward understanding the potential effects of nanoplastics on organisms is to describe the dynamics of ingestion and accumulation at predicted environmental concentrations in seawater (i.e., up to 15 ppb).[10] This has proven to be a difficult analytical challenge. Some studies have attempted to track fluorescent particles using commercially available, manufactured, surface-functionalized polystyrene nanoparticles, to produce qualitative characterization of the ingestion of MP or NP and tissue distributions in relatively transparent aquatic organisms.[11−13] However, the use of fluorescent particles has a number of disadvantages, including high limits of detection (often in the range mg L^{-1}), interferences from fluorescent background signals, the limited range of applicable organisms and rather weak resolution (e.g., due to internal light diffraction/reflection). The challenges of tracking plastic particles in biological or environmental media (including the need for lower limits of detection) have therefore impeded quantification of uptake and accumulation at environmentally realistic concentrations, thus far.

Stable and radioisotope techniques have recently been used successfully to study the fate of nonplastics nanoparticles at environmentally relevant concentrations.[14−16] In principle, this approach could also be used to study fundamental and largely unexplored questions concerning ingestion, depuration and tissue distributions (i.e., translocation) of nanoplastic particles by, and in, organisms.[17] Indeed, radiolabeled nonplastics nanoparticles have been used to overcome the significant limitations for quantifying nanomaterials in environmental and biological media[15,18−20] and to facilitate work at low limits of detection. For instance, radiolabeled silver nanoparticles (*n*Ag) were developed for quantifying and visualizing the distribution of particles in mollusks following exposures at concentrations as low as 100 ng L^{-1} by quantitative whole body autoradiography (QWBA).[14] Such, techniques offer the possibility for direct visualization of intraorgan nanoparticle concentrations. Unfortunately, radiolabeled nanoplastics are not currently available, to our knowledge.

In the present study, we synthesized ^{14}C-labeled nanopolystyrene particles (24 and 250 nm), and then exposed scallops to these particles, measured the biokinetics and quantified NP tissue distributions via QWBA. We used environmentally realistic NP concentrations (15 ppb) to test the hypothesis that this commercially important mollusk might uptake, absorb, and depurate, NP differently according to size. For each particle size, scallops were exposed to a single pulse (6 h) of radiolabeled NP in seawater in the presence of food. Exposed and control animals were sampled over time (i.e., during 48 days) to track NP and to quantify particle distribution.

MATERIALS AND METHODS

Synthesis, Radiolabeling, and Particle Characterizations. Radioactive styrene [methylene-^{14}] (American radiolabeled chemicals Inc., ARC, Saint-Louis, MO) with a nominal specific activity of 2.22 GBq $mmol^{-1}$ was used to synthesize two batches of spherical polystyrene nanoparticles with sizes of approximately 24 ± 13 and 248 ± 21 nm, hereafter described as nPS$_{24}$ and nPS$_{250}$, following the procedures used by Ming et al.[21] and Telford et al.,[22] respectively, for synthesis of nonradiolabeled nanopolystyrene (*n*PS). As the behavior of nanoparticles can be influenced by their shape, spherical *n*PS were prepared so as to be comparable with most previous laboratory-based studies on uptake of plastic particles (SI Figure S1). Unreacted monomer was removed by ultrafiltration (exclusion size of membrane: 30 000 g mol^{-1}). The average size and ζ-potential and the polydispersity index (PDI) of the polymer particles were measured using a multiangle Nicomp ZLS Z3000 (Particle Sizing System, Port Richey, FL). Particle morphology was observed by transmission electron microscopy (TEM; JEOL 1400), at an accelerating voltage of 80 kV. Composition was characterized by Fourier Transform InfraRed spectroscopy (Alpha II FTIR, Bruker).

Organisms. *Pecten maximus* (n = 108, hermaphrodite, shell height 115 ± 16 mm and width 100 ± 13 mm, soft tissue weight 73 ± 16 g), were collected by divers in Plymouth Sound (United Kingdom, 50° 21.292' N, 004° 09.474' W). Before the experiment, the scallops were acclimated for 2 weeks in a 400 L aquarium provided with running seawater (flow rate about 10 L min^{-1}). Water temperature was 12−13 °C and salinity 30−32 PSU throughout acclimation and experiment periods. Scallops were fed daily with a suspension of phytoplankton, which was a mix of *Isochrysis* spp., *Pavlova* spp., *Tetraselmis*, *Chaetoceros calcitrans*, *Thalassiosira weissflogii*, and *Thalassiosira pseudonana* (2×10^9 cells mL^{-1}; ca. 4−20 μm, shellfish diet 1800) at 3% of the dry weight of the animal tissue. The wet weight of each individual was recorded before the start of the exposures.

Exposure Protocol. Scallops were starved for 2 days prior to exposure. A mixture of algae and radioactive *n*PS (either nPS$_{24}$ or nPS$_{250}$) was added to glass aquaria (50 L containing 20 L of aerated and filtered seawater) 1.5 h and 45 min, respectively, before adding groups of 12 scallops. Nominal ^{14}C water concentrations were 5 kBq ^{14}C L^{-1}, which represented 15 μg L^{-1} of *n*PS. The scallops were given a 6 h pulse exposure. Subsequently, scallops were placed in clean 60 L tanks with flowing seawater for a depuration period of 48 days. Temperature, salinity, and daily feeding were maintained as above.

Liquid Scintillation Counting (LSC). Samples of water and soft tissue of scallops were collected during the 6 h uptake period in order to determine a mass balance between water and tissue. Radioactivity in the water was measured in a 10 mL sample using LSC at 1, 2, 3, 4.5, and 6 h. Scallop soft-tissue

DOI: 10.1021/acs.est.8b05266
Environ. Sci. Technol. 2018, 52, 14480−14486

was sampled at 2, 4.5, and 6 h. On each occasion, samples were collected in triplicate. ^{14}C-activity was also measured during the depuration period in the scallops at 1, 2, 3, 8, 14, 24, and 48 days. Soft-tissues were removed from the shells and digested according to the method of Thomson and Burns.[23] Prior to total ^{14}C-measurements by LSC, 10 mL of Ultima Gold cocktail was added to each sample (including water and soft tissue samples) and samples were kept in the dark for 24 h to avoid any chemioluminescence quenching. Samples were measured using a Hidex 300SL counter at the Gordon Institute, University of Cambridge (U.K.), (10 min counting time, minimum detectable activity (MDA) = limit of detection (LOD) 0.08 Bq mL^{-1}; SI eq S1). Background count rates were determined by counting samples from the control exposure (i.e., water and scallops from aquaria to which no *n*PS particles had been added).

Quantitative Whole-Body Autoradiography (QWBA). The distribution of particles in tissues was visualized using QWBA on two scallops from each group at the end of the exposure period (i.e., after 6 h of uptake), after 8 days of depuration and after 48 days of depuration. Soft tissues were detached from the shell, embedded in a 2.5% (p/v) aqueous gel of carboxymethylcellulose and flash-frozen in liquid nitrogen. The resulting block was cut at −25 °C with a specially designed cryomicrotome (Leica CM3600). A pair of 50 μm thick tissue sections was collected every 0.75 mm, freeze-dried and exposed for 3 weeks on a phosphor screen. The screens were scanned with a phosphor imager Typhoon FLA7000 (GE Healthcare) to obtain images of the ^{14}C distribution. Areas of interest were isolated, and radioactivity quantified as digital light unit per mm^2 of tissue section (DLU mm^{-2}) with ImageJ. These values were corrected for exposure time on phosphor screens, normalized for an exposure concentration of 5 kBq L^{-1} and expressed as a signal/noise ratio (S/N) to correct for background BG (in DLU mm^{-2} h^{-1}) as described by Al-Sid-Cheikh et al.[14] using R script treatment. Calibration blood dots were added to each screen to permit quantification in units of Bq g^{-1}, ng g^{-1} and particles g^{-1}.

Kinetic Models of Accumulation. Accumulation in the animal (dC_A/dt) is related to the concentration in water (C_W), and an uptake rate constant (k_{upt}) and can be expressed as

$$\left[\frac{dC_A}{dt}\right] = k_{upt} \cdot C_W$$

Elimination was modeled according to the following biexponential equation:

$$C_t = [C_1 \cdot e^{-k_{e1}t}] + [C_2 \cdot e^{-k_{e2}t}]$$

where C_t corresponds to the percentage of radioactivity remaining at time t, relative to radioactivity measured at t_0; C_1 and C_2 represent the percentage of radioactivity in the fast (C_1) and slow (C_2) kinetics compartments at t_0 ($C_1 + C_2 = t_0 = 100$); k_{e1} and k_{e2} correspond to the elimination rates in the fast and slow kinetics compartments, respectively. Uptake and elimination parameters (i.e., k_{upt}, C_1, C_2, k_{e1} and k_{e2}) were determined using the method of Borretzen and Salbu,[24] as described by Al-Sid-Cheikh et al.[14] using R. The long-term bioconcentration factor (BCF) of ^{14}C, nPS$_{24,\ 250}$ was modeled as described by Al-Sid-Cheikh et al.[14] BCF is the quantity of NP in each scallop at time t expressed as a bioconcentration factor. All k_{upt} of ^{14}C were compared between groups using *t* tests.

RESULTS

Uptake. Both 24 and 250 nm nanopolystyrene (*n*PS) accumulated in *P. maximus* during the pulse exposures (Figure 1a). During this 6 h period, the scallops accumulated 30% and

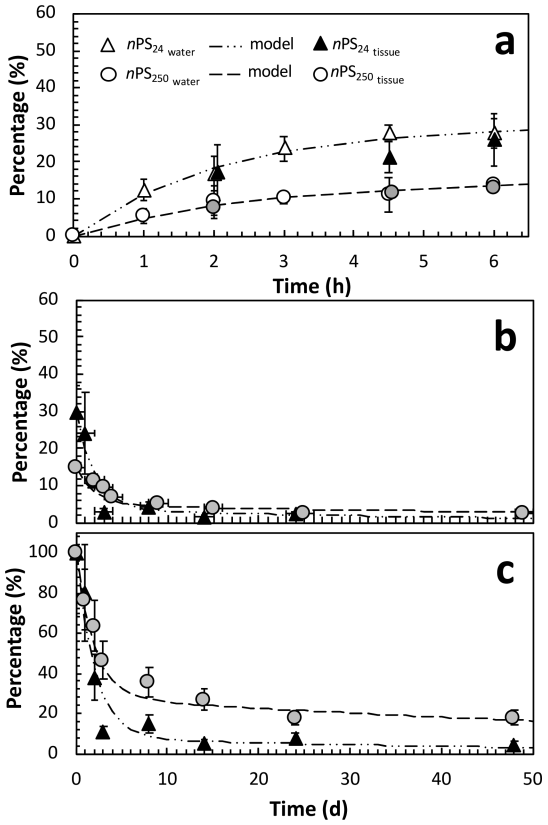

Figure 1. Biokinetics of uptake and depuration of 24 and 250 nm nanopolystyrenes. (a) ^{14}C-levels expressed as a percentage of radioactivity relative to ^{14}C spiked at t_0 in the aquarium; open symbols represent the activity removed from the water (mean ± SD, n = 3) and solid symbols the total activity measured in the scallops (mean ± SD, n = 3) and (b) nPS$_{24,250}$ levels (i.e., solid black triangle and solid gray circle, respectively), expressed as % radioactivity (in tissue) remaining relative to maximum available in the aquarium during the uptake, (c) nPS$_{24,250}$ levels (same legend as a and b), expressed as % radioactivity remaining relative to depuration t = 0 (mean ± S.D., n = 3). Data are also shown in SI Table S1.

15% of the available NP burden in the medium, for nPS$_{24}$ and nPS$_{250}$, respectively (Figure 1a, SI Table S1). The data shown in Figure 1a indicate that nPS$_{24}$ was taken up 2.5 times faster (p-value < 0.001, t test, n = 6) than nPS$_{250}$ with uptake values of 0.5 ± 0.08 and 0.2 ± 0.01 Bq h^{-1} (SI Table S2), respectively. Consequently, at these rates, the accumulation capacity (i.e., here define as 95% of the scallop capacity) would be reached after 11 and 30 h of continued exposures for nPS$_{24}$ and nPS$_{250}$ ($t_{0.95}$, SI Table S2), respectively.

Depuration. For both particle sizes, the majority of *n*PS were depurated within 3 days (Figure 1b, c). Specifically, during the first compartment of depuration, 88 and 68% of the initial burdens were purged for nPS$_{24}$ and nPS$_{250}$, respectively, with a similar elimination rate (k_{e1}) and biological half-life ($t_{1/2}$) of about 1.4 days (Table S3). The main difference between particle sizes occurred during the subsequent depuration compartment, where the rates ($k_{e2;}$ $t_{1/2}$ = 35 and 64 d) were 25 and 50 times slower than for the first stage (k_{e1})

DOI: 10.1021/acs.est.8b05266
Environ. Sci. Technol. 2018, 52, 14480−14486

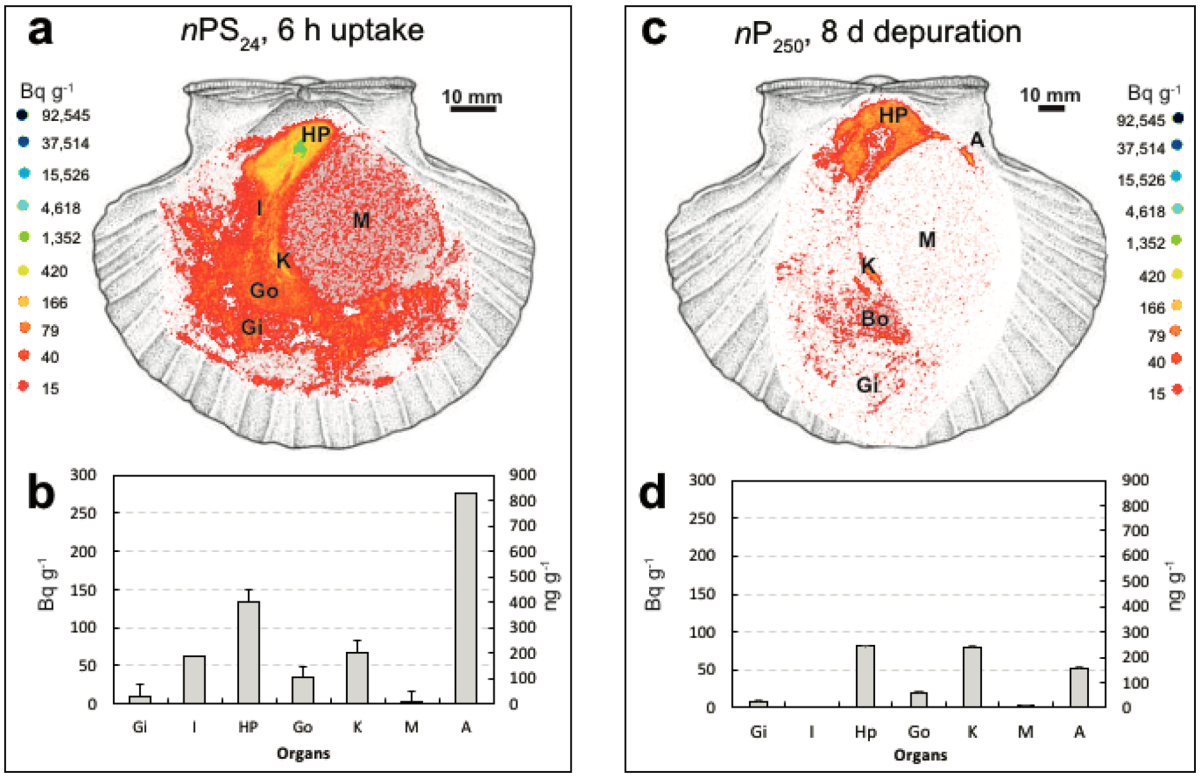

Figure 2. Uptake and depuration of 24 nm polystyrene nanoparticles. (a) Tissue distributions shown by Quantitative Whole Body autoradiography (QWBA) in *Pecten maximus* after 6 h uptake (section photo SI Figure S3a) with (b) quantification of radioactivity levels) measured in tissues (left axis; Bq g^{-1}, S/N_{norm}; right axis ng g^{-1}), (c) Tissue distributions shown by Quantitative Whole Body autoradiography (QWBA) in *Pecten maximus* after 8 days of depuration (section photo SI Figure S3b), with (d) quantification after 8 days of depuration (left axis Bq g^{-1}, S/N_{norm}; right axis, ng g^{-1}). Each bar represents the mean value measured in 3−6 different sections of a given individual. No bar = radioactivity < LOD. HP: Hepatopancreas, Gi: Gills, Go: Gonad, I: Intestine, K: Kidney, M: Muscle, A: Anus.

for nPS$_{24}$ and nPS$_{250}$, respectively. That is, depuration kinetics were slower for nPS$_{250}$ than for nPS$_{24}$. The LSC limit of detection was reached after 14 days of depuration for nPS$_{24}$ particles, while nPS$_{250}$ particles were still detectable after 48 day depuration (Figure 1b, c).

Tissue Distributions. The distribution of nPS$_{24}$ within scallops after the 6 h exposure to a single pulse was revealed by QWBA (Figure 2a; SI Figures S3 and S4). Quantification showed that after 6 h, nPS$_{24}$ was distributed in the hepatopancreas (1579.5 ± 35 ng), gills (1385.7 ± 400 ng), gonad (913.9 ± 16 ng), muscle (863.0 ± 19 ng, kidney (328.7 ± 15 ng), intestine (226.8 ± 16 ng), and anus (163. Two ±22 ng) (Figure 2b, SI Table S4). After 8 days of elimination, nPS$_{24}$ was still detectable (Figure 2c). The amounts remaining at this stage (Figure 2d, SI Table S4) were 556.8 ± 171 ng (gills), 324.6 ± 31 ng (hepatopancreas), 149.6 ± 211 ng (muscle), 148.7 ± 97 ng (gonads), 35.9 ± 24 ng (kidney), and 13.0 ± 18.4 ng (anus). After 14 days, ^{14}C levels of nPS$_{24}$ were below the limit of detection of QWBA, in agreement with the LSC measurements. The activity recorded by QWBA for scallops exposed to nPS$_{250}$ was significantly lower than those for nPS$_{250}$ (consistent with slower and reduced uptake of nPS$_{250}$ of this size) and was only detectable as a single spot of activity in the intestine (SI Figure S2). Any activity in the anus, hepatopancreas, kidney, intestine, gonad, gills, and muscle was below the limit of detection.

Bioaccumulation. Long-term chronic exposure model predictions were generated from the results of the single-pulse experiment. Bioconcentration factors (BCF) representing the quantity of nPS$_{24}$ and nPS$_{250}$ in the scallops at time t, expressed as the BCF in mL exposure water g^{-1}_{ww}, (as indicated in Materials and Methods), were calculated. The model outputs indicated (Figure 3; SI Figure S4), that the

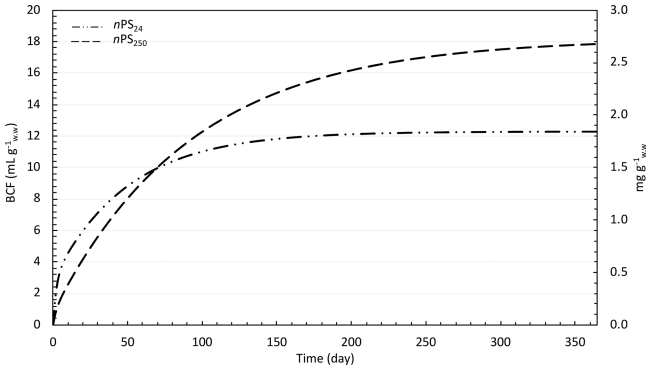

Figure 3. Long-term biokinetics model for accumulation over a one year of exposure to a constant seawater concentration of 15 μg L^{-1} (ppb) nPS. The long-dash-dot-dot curve represents accumulation of 24 nm and the dashed curve 250 nm nPS.

concentration of nPS$_{24}$ in the scallops would increase faster than nPS$_{250}$ during the first 60−100 days of exposure and would then reach a steady state after around 200 d. BCF$_{250}$ was calculated to increase more slowly in the first 60−70 days but was predicted to reach a steady-state after around 300 days (Figure 3). Bioaccumulation modeling predicted that during

DOI: 10.1021/acs.est.8b05266
Environ. Sci. Technol. 2018, 52, 14480−14486

chronic exposures, nPS$_{250}$ would become more bioconcentrated in *P. maximus* than nPS$_{24}$. Consequently, the predicted concentrations (Figure 3) after a year would be 1.8 and 2.7 mg g^{-1} (wet weight) for nPS$_{24}$ and nPS$_{250}$ in *P. maximus*, for a constant environmental concentration of 15 μg L^{-1}. Alternatively, when the model is applied to a constant environmental concentration of 100 ng L^{-1} instead, the predicted concentration accumulated by *P. maximus* decreased to 12 and 18 μg g^{-1} for nPS$_{24}$ and nPS$_{250}$, respectively. At a concentration of 1 pg L^{-1}, the model predicted tissue concentrations of 123 and 178 ng g^{-1}, for nPS$_{24}$ and nPS$_{250}$, respectively.

DISCUSSION

Environmentally Relevant Concentrations. This study reports biokinetic and tissue distribution data for nPS at what have been predicted previously as possible environmentally realistic concentrations of nanoplastics.[9] Use of radiolabeled nanoparticles allowed demonstration of tissue distributions and biokinetics. By exposing scallops to a single pulse of nPS particles, our experiments showed that even at a concentration of 15 μg L^{-1}, plastic particles accumulated rapidly in the scallop (Figure 1a). Once transferred to clean seawater, the radioactive particles were depurated relatively rapidly (Figure 1b). The potential for some nPS$_{24}$ detectable by QWBA, but not detectable nPS$_{250}$ particles, to transfer via the circulatory system is also suggested somewhat by the data, which apparently show the presence of nPS$_{24}$ in muscles. This emphasizes the advantages of using radiolabeling techniques. These may now be used to investigate the distribution of NP particles at relatively low concentrations to other organisms and during longer-term exposures in order to reach steady states at environmentally realistic concentrations and with modeling perhaps to provide useful information on the potential chronic fate of NP.

Ingestion of Nanopolystyrene. Bivalves are generally capable of discriminating between algal cells of different sizes by a pseudofeces rejection mechanism.[25] The retention pattern for particles below 5−7 μm varies somewhat between species. For example, *Chlamys islandica* is more efficient in capturing small particles than *Chlamys opercularis*.[25] Some scallops, such as Pectinidae, are capable of ingesting larger particles (up to 950 μm[26]). This ability has been related to the apparent absence of a sorting mechanism based on particle sizes.[27] Nevertheless, an upper limit for capture/ingestion of particles of approximately 20 μm for adult scallops has been suggested.[28] Our experiments show a size effect at much smaller sizes, on the uptake rate of nPS by *P. maximus*. nPS$_{24}$ was taken up 2.5 times faster than nPS$_{250}$. These results are in agreement with a previous experiment exposing 20 and 80 nm radiolabeled silver nanoparticles (i.e., n^{110m}Ag$_{20-80}$) to the scallop *C. islandica* under similar conditions.[14] Indeed, nPS$_{24}$ accumulated at a similar rate to n^{110m}Ag$_{20}$, while n^{110m}Ag$_{80}$ was ingested at a slower rate than observed for nPS$_{250}$. Three levels of specialization are generally suggested to explain the variability in particle processing by bivalves: morphological (different pallial organ configurations corresponding to differences in processing sites and mechanisms), biochemical (different mucopolysaccharide types accomplishing different processing functions) and ciliary, with specific ciliary types affecting different functions, such as particle interception or various types of transport.[29] We suggest that one, or all, these mechanisms (most probably pallial organ configuration and a ciliary level of specialization), may be less effective for nanoscale particles. The difference between the ingestion rate of smaller and larger nPS could possibly also be explained by differences in sedimentation and agglomeration rates of the particles, which would affect their availability to the scallops. For example, Ward and Kach[30] observed that marine aggregates facilitated the ingestion of nPS$_{100}$ in oysters and mussels. In a similar way, White[31] (1997) found that flocculation increased the ability of adult *Placopecten magellanicus* to retain small (<7 μm) clay particles. If the smaller nPS agglomerate and precipitate faster than the bigger NP, smaller nPS might have become more accessible to the scallop. Recently, it has been suggested that bivalves might also uptake plastic particles through adherence, in addition to traditional ingestion.[32] This alternative absorption mechanism is likely to occur during quick depuration processes and indicates that plastic particles could relocate in bivalves via the action of the foot and the mantle.

Depuration of Nanopolystyrene. Particle selection in the gut or in the digestive gland-stomach of bivalves is complex and not well understood. It is thought that some bivalves can discriminate among particles in the gut and can preferentially adsorb nutritional particles.[33−35] Post ingestion discrimination is thought to occur, either by the preferential retention of some particles in the stomach, allowing more time for extracellular digestion, or by the direction of some particles toward the digestive gland for intracellular digestion.[25] In the present experiment, the first step of the depuration process (i.e., where more than 65% of the initial burden was purged), showed relatively high depuration rates; approximately 13 times faster for both sizes of nPS than those previously observed with n^{110m}Ag$_{20}$[14]. *P magellanicus* has, for example, been shown to distinguish between particles of different size and density and to retain larger and lighter particles longer.[36] Such size and composition selection require energy consumption. However, little is known about the associated energy costs.[25] Nevertheless, the presence of NP might represent an important energy cost. For example, in bivalves such as *Mytilus edulis*, the excretory loss of nitrogenous products can represent up to 31% of respiratory energy demand.[37]

Tissue Distribution of Particles. Tissue distribution is of key importance for evaluation of the potential for particles translocation within an organism and thus for future understanding of any toxicological effects and transfer within the food web.[38] Translocation may increase residence time, bioaccumulation and create long-term effects in organisms.[17] Fluorescent labeling has been widely used to track contaminants in environmental compartments (e.g., refs 11 and 39). However, this approach has major restrictions, such as the limit of detection, the type of organisms that can be used (i.e., a relatively transparent organisms), fluorescent responses from background material and the poor optical resolution (e.g., due to internal light diffraction/reflection). Studies have produced qualitative characterization of ingestion of MP/NP in relatively transparent organisms.[11−13] The tissue distribution of nPS$_{24}$ in *Pecten maximus* suggests ingestion and accumulation in the digestive cavity and tubules and translocation into the circulatory system from which radioactive particles reached the gonad, kidney and muscle (Figure 2). The presence of NP in muscle tissue perhaps indicates that some particles had crossed epithelial membranes. Our results with nPS$_{24}$ show contrasting tissue distributions to previous observations with n^{110m}Ag$_{20}$, which were mostly distributed in the hepatopancreas (including a "hot spot" in the gastric shield). This

DOI: 10.1021/acs.est.8b05266
Environ. Sci. Technol. 2018, 52, 14480−14486

comparison between nanoparticles of similar sizes, but different compositions (nanopolystyrene versus nanosilver), suggests that tissue distributions might be influenced by the type of nanoparticles. These observations suggest that the chemical composition of the nanomaterials may have important effects on their behavior in biological systems, perhaps due to differences in physical chemistry. The relatively homogeneous distribution of $n\mathrm{PS}_{24}$ compared to that observed for $n^{110m}\mathrm{Ag}_{20}$, as well as the relatively higher accumulation of $n\mathrm{PS}_{24}$ than $n\mathrm{PS}_{250}$ in the hepatopancreas and kidney and its rapid disappearance from the gills, suggest stronger translocation of $n\mathrm{PS}_{24}$ than $n\mathrm{PS}_{250}$ and different depuration mechanisms. Nanoparticles are likely to follow the same uptake routes as suspended food particles, which are normally trapped in mucus and transported toward the digestive gland by ciliary action.[29] The binding of $n\mathrm{PS}_{24,250}$ by mucus proteins and transport by this same route cannot be excluded, but it is not possible with the present data to determine the contribution of this route compared to possible uptake via the gills. Furthermore, contrary to previous work with $n^{110m}\mathrm{Ag}_{20}$, the presence of $n\mathrm{PS}_{24}$ in kidney, heart, and muscle suggests possible translocation to the circulatory system, which might be explained by capability to cross-epithelial walls and cell membranes (i.e., lipid membranes)[40] or indirect transportation by hemocytes after absorption.[41]

■ ASSOCIATED CONTENT

Supporting Information

The Supporting Information is available free of charge on the ACS Publications website at DOI: 10.1021/acs.est.8b05266.

A plot of studies targeting micro- and nanoplastics reported in the literature. Quantitative whole-body autoradiography (QWBA) and section photo for $n\mathrm{PS}_{250}$ after 6 h uptake. Photography of section used for the QWBA image for $n\mathrm{PS}_{24}$ after 6 h uptake and 8 days of depuration. Biokinetic parameters measured for $n\mathrm{PS}_{24}$ and $n\mathrm{PS}_{250}$. Uptake and depuration total activity $^{14}\mathrm{C}$ and conversion in mass per grams of biological tissue (wet weight). Kinetic parameter of elimination. QWBA quantification of $n\mathrm{PS}_{24}$ after 6 h uptake and 8 day depuration (PDF)

■ AUTHOR INFORMATION

Corresponding Authors

*(M.A.-S.-C.) Phone: +44(0)1 752 585 913; e-mail: maya.al-sid-cheikh@plymouth.ac.uk.

*(R.C.T.) Phone: +44(0)1 1752 584651; e-mail: R.C.Thompson@plymouth.ac.uk.

ORCID

Maya Al-Sid-Cheikh: 0000-0003-3558-1733

Theodore B. Henry: 0000-0002-9675-9454

Notes

The authors declare no competing financial interest.

■ ACKNOWLEDGMENTS

We thank the University of Plymouth dive team (R. Sandercock, M. Brown, C. Sandercock, R. Gannon, and R. Lilley) for collecting the scallops and R. Haslam, R. Ticehirst, and M. Palmer For technical support. We thank the University of Plymouth and staff for access to the Consolidated Radioisotope Facility, (W. Blake, A. Taylor, G. Millward, and N. Crocker). We thank A. Bannister from the Gordon Institute, University of Cambridge, for access to a liquid scintillation counter. We also thank M-A. Cormier for his help during the exposure experiments and D. Koseoglu for his help with use of ImageJ and R. We thank Peter Bond and Glenn Harper of Plymouth Electron Microscopy Centre (PEMC) for their support and assistance in this work. This research was part of the RealRiskNano project funded by the Natural Environment Research Council, UK, (grant number: NE/N006526/1).

■ REFERENCES

(1) PlasticsEurope. *Plastics – the Facts 2017, An Analysis of European Plastics Production, Demand and Waste Data*; Brussels, Belgium, 2018.

(2) Thompson, R. C.; Olsen, Y.; Mitchell, R. P.; Davis, A.; Rowland, S. J.; John, A. W. G.; McGonigle, D.; Russell, A. E. Lost at Sea: Where Is All the Plastic? *Science (Washington, DC, U. S.)* **2004**, *304* (5672), 838.

(3) Van Sebille, E.; Wilcox, C.; Lebreton, L.; Maximenko, N.; Hardesty, B. D.; Van Franeker, J. A.; Eriksen, M.; Siegel, D.; Galgani, F.; Law, K. L. A Global Inventory of Small Floating Plastic Debris. *Environ. Res. Lett.* **2015**, *10* (12).124006

(4) Koelmans, A. A.; Besseling, E.; Shim, W. J. Nanoplastics in the Aquatic Environment. Critical Review. In *Marine Anthropogenic Litter*; Bergmann, M., Gutow, L., Klages, M., Eds.; Springer International Publishing: Cham, 2015; pp 325–340.

(5) Lambert, S.; Wagner, M. Characterisation of Nanoplastics during the Degradation of Polystyrene. *Chemosphere* **2016**, *145*, 265–268.

(6) Gigault, J.; Pedrono, B.; Maxit, B.; Ter Halle, A. Marine Plastic Litter: The Unanalyzed Nano-Fraction. *Environ. Sci.: Nano* **2016**, *3* (2), 346–350.

(7) Vance, M. E.; Kuiken, T.; Vejerano, E. P.; McGinnis, S. P.; Hochella, M. F., Jr.; Rejeski, D.; Hull, M. S. Nanotechnology in the Real World: Redeveloping the Nanomaterial Consumer Products Inventory. *Beilstein J. Nanotechnol.* **2015**, *6*, 1769–1780.

(8) Hernandez, L. M.; Yousefi, N.; Tufenkji, N. Are There Nanoplastics in Your Personal Care Products? *Environ. Sci. Technol. Lett.* **2017**, *4* (7), 280–285.

(9) Lenz, R.; Enders, K.; Nielsen, T. G. Microplastic Exposure Studies Should Be Environmentally Realistic. *Proc. Natl. Acad. Sci. U. S. A.* **2016**, *113* (29), E4121–E4122.

(10) Renner, G.; Schmidt, T. C.; Schram, J. Analytical Methodologies for Monitoring Micro(Nano)Plastics: Which Are Fit for Purpose? *Curr. Opin. Environ. Sci. Heal.* **2018**, *1*, 55–61.

(11) Cole, M.; Lindeque, P.; Fileman, E.; Halsband, C.; Goodhead, R.; Moger, J.; Galloway, T. S. Microplastic Ingestion by Zooplankton. *Environ. Sci. Technol.* **2013**, *47* (12), 6646–6655.

(12) Cui, R.; Kim, S. W.; An, Y.-J. Polystyrene Nanoplastics Inhibit Reproduction and Induce Abnormal Embryonic Development in the Freshwater Crustacean Daphnia Galeata. *Sci. Rep.* **2017**, *7* (1), 12095.

(13) Ma, Y.; Huang, A.; Cao, S.; Sun, F.; Wang, L.; Guo, H.; Ji, R. Effects of Nanoplastics and Microplastics on Toxicity, Bioaccumulation, and Environmental Fate of Phenanthrene in Fresh Water. *Environ. Pollut.* **2016**, *219*, 166–173.

(14) Al-Sid-Cheikh, M.; Rouleau, C.; Pelletier, E. Tissue Distribution and Kinetics of Dissolved and Nanoparticulate Silver in Iceland Scallop (Chlamys Islandica). *Mar. Environ. Res.* **2013**, *86*, 21–28.

(15) Al-Sid-Cheikh, M.; Pelletier, É.; Rouleau, C. Synthesis and Characterization of [110mAg]-Nanoparticles with Application to Whole-Body Autoradiography of Aquatic Organisms. *Appl. Radiat. Isot.* **2011**, *69* (10), 1415–1421.

(16) Laycock, A.; Stolpe, B.; Römer, I.; Dybowska, A.; Valsami-Jones, E.; Lead, J. R.; Rehkämper, M. Synthesis and Characterization of Isotopically Labeled Silver Nanoparticles for Tracing Studies. *Environ. Sci.: Nano* **2014**, *1* (3), 271–283.

(17) Browne, M. A.; Dissanayake, A.; Galloway, T. S.; Lowe, D. M.; Thompson, R. C. Ingested Microscopic Plastic Translocates to the

DOI: 10.1021/acs.est.8b05266
Environ. Sci. Technol. 2018, 52, 14480–14486

Circulatory System of the Mussel, Mytilus Edulis (L.). *Environ. Sci. Technol.* **2008**, *42* (13), 5026−5031.
(18) Petersen, E. J.; Huang, Q.; Weber, W. J. J. Ecological Uptake and Depuration of Carbon Nanotubes by Lumbriculus Variegatus. *Environ. Health Perspect.* **2008**, *116* (4), 496−500.
(19) Georgin, D.; Czarny, B.; Botquin, M.; Mayne-L'Hermite, M.; Pinault, M.; Bouchet-Fabre, B.; Carriere, M.; Poncy, J.-L.; Chau, Q.; Maximilien, R.; Dive, V.; Taran, F. Preparation of 14C-Labeled Multiwalled Carbon Nanotubes for Biodistribution Investigations. *J. Am. Chem. Soc.* **2009**, *131* (41), 14658−14659.
(20) Lanctôt, C. M.; Al-Sid-Cheikh, M.; Catarino, A. I.; Cresswell, T.; Danis, B.; Karapanagioti, H. K.; Mincer, T.; Oberhänsli, F.; Swarzenski, P.; Tolosa, I.; Metian, M. Application of Nuclear Techniques to Environmental Plastics Research. *J. Environ. Radioact.* **2018**, *192*, 368−375.
(21) Ming, W.; Zhao, J.; Lu, X.; Wang, C.; Fu, S. Novel Characteristics of Polystyrene Microspheres Prepared by Microemulsion Polymerization. *Macromolecules* **1996**, *29* (24), 7678−7682.
(22) Telford, A. M.; Pham, B. T. T.; Neto, C.; Hawkett, B. S. Micron-Sized Polystyrene Particles by Surfactant-Free Emulsion Polymerization in Air: Synthesis and Mechanism. *J. Polym. Sci., Part A: Polym. Chem.* **2013**, *51* (19), 3997−4002.
(23) Thomson, J.; Burns, A. D. *CS-003: LSC Sample Preparation by Solubilization*; Torrance, CA, 2008; 2p.
(24) Børretzen, P.; Salbu, B. Bioavailability of Sediment-Associated and Low-Molecular-Mass Species of Radionuclides/Trace Metals to the Mussel Mytilus Edulis. *J. Environ. Radioact.* **2009**, *100* (4), 333−341.
(25) MacDonald, B. A.; Monica Bricelj, V. Chapter 7 Physiology: Energy Acquisition and Utilisation. *Dev. Aquacult. Fish. Sci.* **2006**, *35*, 417−492.
(26) Mikulich, L. V.; Tsikhon-Lukanina, A. Food of the Scallop. *Oceanology* **1981**, *21* (5), 633−635.
(27) Beninger, P. G.; Le Pennec, M.; Salaün, M. New Observations of the Gills of Placopecten Magellanicus (Mollusca: Bivalvia), and Implications for Nutrition - I. General Anatomy and Surface Microanatomy. *Mar. Biol.* **1988**, *98* (1), 61−70.
(28) Kingzett, B. C. *Ontogeny of Suspension Feeding in Post-Metamorphic Japanese Scallops, Patinopecten yessoensis (Jay)*; Acquisitions and Bibliographic Services Branch, National library of Canada: Ottawa, 1993.
(29) Beninger, P.; St-Jean, S.; Poussart, Y.; Ward, J. Gill Function and Mucocyte Distribution in Placopecten Magellanicus Ana Mytilus Edulis (Mollusca: Bivalvia): The Role of Mucus in Particle Transport. *Mar. Ecol.: Prog. Ser.* **1993**, *98*, 275−282.
(30) Ward, J. E.; Kach, D. J. Marine Aggregates Facilitate Ingestion of Nanoparticles by Suspension-Feeding Bivalves. *Mar. Environ. Res.* **2009**, *68* (3), 137−142.
(31) White, M. J. *The Effect of Flocuculation on the Size-Selective Feeding Capabilities of the Sea Scallop Placopecten Magellanicus*; Nova Scotia: Halifax, 1997.
(32) Kolandhasamy, P.; Su, L.; Li, J.; Qu, X.; Jabeen, K.; Shi, H. Adherence of Microplastics to Soft Tissue of Mussels: A Novel Way to Uptake Microplastics beyond Ingestion. *Sci. Total Environ.* **2018**, *610−611*, 635−640.
(33) Shumway, S. E.; Cucci, T. L.; Newell, R. C.; Yentsch, C. M. Particle Selection, Ingestion, and Absorption in Filter-Feeding Bivalves. *J. Exp. Mar. Biol. Ecol.* **1985**, *91* (1−2), 77−92.
(34) Lopez, G. R.; Levinton, J. S. Ecology of Deposit-Feeding Animals in Marine Sediments. *Q. Rev. Biol.* **1987**, *62* (3), 235−260.
(35) Bayne, B. L.; Hawkins, A. J. S.; Navarro, E.; Heral, M.; Deslous-Paoli, J. M. Feeding Behaviour of the Mussel, Mytilus Edulis: Responses to Variations in Quantity and Organic Content of the Seston. *J. Mar. Biol. Assoc. U. K.* **1993**, *73* (4), 813−829.
(36) Brillant, M. G. S.; MacDonald, B. A. Postingestive Selection in the Sea Scallop, Placopecten Magellanicus (Gmelin): The Role of Particle Size and Density. *J. Exp. Mar. Biol. Ecol.* **2000**, *253* (2), 211−227.
(37) Hilbish, T. J.; Koehn, R. K. The Physiological Basis of Natural Selection at the Lap Locus. *Evolution (Hoboken, NJ, U. S.)* **1985**, *39* (6), 1302−1317.
(38) Martin, J. W.; Mabury, S. A.; Solomon, K. R.; Muir, D. C. G. Bioconcentration and Tissue Distribution of Perfluorinated Acids in Rainbow Trout (*Oncorhynchus Mykiss*). *Environ. Toxicol. Chem.* **2003**, *22* (1), 196−204.
(39) Cole, M.; Galloway, T. S. Ingestion of Nanoplastics and Microplastics by Pacific Oyster Larvae. *Environ. Sci. Technol.* **2015**, *49* (24), 14625−14632.
(40) Rossi, G.; Barnoud, J.; Monticelli, L. Polystyrene Nanoparticles Perturb Lipid Membranes. *J. Phys. Chem. Lett.* **2014**, *5* (1), 241−246.
(41) Cajaraville, M. P.; Pal, S. G. Morphofunctional Study of the Haemocytes of the Bivalve Mollusc Mytilus Galloprovincialis with Emphasis on the Endolysosomal Compartment. *Cell Struct. Funct.* **1995**, *20* (5), 355−367.

DOI: 10.1021/acs.est.8b05266
Environ. Sci. Technol. 2018, 52, 14480−14486